



## Helmholtz Hamiltonian Mechanics Electromagnetic Physics Gaging Charge Fields Having Novel Quantum Circuitry Model

RAJAN IYER<sup>1</sup>, CHRISTOPHER O'NEILL<sup>2</sup> and MANUEL MALAVER<sup>3\*</sup>

<sup>1</sup>Engineering International Operational Teknet Earth Global, Department of Physical Mathematics Sciences Engineering Project Technologies, Tempe, Arizona, United States of America.

<sup>2</sup>Cataphysics Group, Ireland.

<sup>3</sup>Maritime University of the Caribbean, Department of Basic Sciences, Catia la Mar, Venezuela.

### Abstract

This article shows novel model Pauli-Dirac-Planck-quantum-circuit-assembly-gage, consisting of the monopole quasiparticles and electron-positron particle fields, demonstrating power of Iyer Markoulakis Helmholtz Hamiltonian mechanics of point vortex and gradient fields general formalism. Transforming this general metric to Coulombic gaging metrics and performing gage charge fields calculations, derivation of assembly eigenvector matrix bundle constructs of magnetic monopoles, and electron positron particle gage metrics were successfully compiled, like SUSY  $\begin{pmatrix} 1 & \epsilon \\ \epsilon^* & 1 \end{pmatrix}$  Hermitian quantum matrix., modified to asymmetric strings gage metrics to account for asymmetrical magnetic pole forces measurements recently in physics. Physical analysis with graphics discussing scenarios of electric tensor particles and magnetic tensor monopoles permutationally interacting, figures showing simulations of fermions' spins with Clifford algebraic geometry, and the graphs explaining vortex sinusoidal pulsed signal output distribution profile of typical equivalent wave velocity of the related point fields partially verify this quantum circuitry assembly model. Table shows estimated size of this assembly greater than  $10^{-34}$  Planck unit and less than quasi-particle size of  $10^{-26}$  metrics unit. Wide-ranging applications of this quantum circuitry assembly model exist for quantum supercomputing expertise antenna networks, alongside quantum astrophysical grand unifying genesis of electromagnetic gravitational matter antimatter systems. This quantum model can be verified by experimental techniques, such as spin-ice and Bose-Einstein condensate spinors.



### Article History

Received: 18 August 2021

Accepted: 18 October 2021

### Keywords

Asymmetric Strings Gage Metrics,  
Electromagnetism;  
Gage;  
Helmholtz Hamiltonian Mechanics;  
Monopoles;  
Physics;  
Particles;  
Pauli Dirac Planck Circuit Like Monopole Particle Assembly;  
Susy;  
String metrics;  
Transforms;  
Quantum Computers.

**CONTACT** Manuel Malaver ✉ mmf.umc@gmail.com 📍 Maritime University of the Caribbean, Department of Basic Sciences, Catia la Mar, Venezuela.



© 2020 The Author(s). Published by Oriental Scientific Publishing Company

This is an Open Access article licensed under a Creative Commons license: Attribution 4.0 International (CC-BY).

Doi: <http://dx.doi.org/10.13005/OJPS05.01-02.06>

## Introduction

Point fields have been modeled applying Helmholtz decomposition matrix of gradient fields and rotational vortex fields, based on real time observational measurements with Ferrocens<sup>1</sup> {<sup>1</sup>Commercially known as a Ferrocell. Ferrocell@USA Trademark. US Patent 8246356 "Magnetic flux viewer". Website: <https://www.ferrocell.us/>} of a synthetic magnetic monopole assembly magneton.<sup>1,2</sup> Iyer Markoulakis Helmholtz Hamiltonian quantum mechanical general formalism derived<sup>1</sup> have been applied to solve practical problem of attraction and repulsion of entity point objects, specifically encountered in all electronic and magnetic entity forms, that will include monopoles within a dipole quagmire, by deriving algebraic equations,<sup>3</sup> from the partial differential equations of general formalism.<sup>1</sup> Graphic plots having input vortex signals and output sinusoidal signals showed bunching effects, suggestive of conversion of energy to condensed form like time-crystal physics, with quasi, fermionic, or bosonic type of particles, alongside possibility of existence of a superfluid condensate acting in essence as vacuum quanta quagmire.<sup>3</sup> Sizes of these entities have been estimated to be typically  $10^{-20}$  m, that is many orders of magnitude less than the known sizes of fermions and/or Bohr atom,  $10^{-18}$  m to  $10^{-15}$  m. Analytical interpretation of above computations showed that depending on monopole mass, entity sizes with zero point gradient energy of  $10^{26}$  metric units, sizes of these entities may vary from values of  $10^{-20}$  m or even lesser to  $10^{-18}$  m, especially due to microblackhole mechanism compressing monopole mass from  $10^{-47}$  kg to  $10^{-11}$  kg. With entities propagating away from microblackhole, monopole mass value reducing closer to  $10^{-47}$  kg with evolution of time, continuous propagation of generators assisted by quantum field photon mediators will be expected to create quarks, antiquarks, and the gluons out of vacuum quanta.<sup>3</sup>

Physical mathematical gaging mechanics to electromagnetic theory has gotten facilitated by ansatz formalism that has power to pull out observables with parameters of quantum density matrix operator eigenfunctions having general energy tensor fields,  $E$ , the functional commutator,  $F^{Et}$ , with density matrix,  $\rho(t)$ , influencing time event process. Time fields that are typical of micro-blackholes, shown to be analytically evidenceable from differential equations will determine these processes.<sup>4</sup> Iyer Markoulakis Helmholtz Hamiltonian

general formalisms have been aptly converted to gage matrix,<sup>5</sup> following physics literature procedures. Transformation of Helmholtz metrics to Coulomb gage, linking also Coulomb branch gage group with Hilbert series has also been quantifiably achieved having gradient fields converted to Coulomb gage, with rotational vortex fields branching to Hilbert gauge mass metrics of Higgs-Boson matter, and conforming to partial differential equations of vortex and the gradient fields obtained per Iyer Markoulakis original general formalism,<sup>1,5</sup> Vacuum gravitational solutions of the fields provided means to arrive at unitary determinant that will analytically project to having almost infinite extension of gauge matrix metrics, like stringmetrics construct showing typically charge asymmetry gage metrics.<sup>5</sup> Results of general formalism have been also discussed extensively with Physical Analysis of particle physics gage matrix pointing to Dirac seas of electrons, monopoles with positrons, electron-positron annihilation leading to energy production, and the relativistic energy generating matter. Quantum astrophysics gage matrix proposed mechanism of creation of neutrino antineutrino pair orthogonal to electron positron "curdling" planes, that may lead to the formation of protonic hydrogen of stars or orthogonally to these "curdling" planes muon particles, that are consistent with physics literature, have been elaborated further with concept of the vacuum monopoles posed to occur at extent of infinite cosmos.<sup>1,3,5</sup>

Gage conversions are quite useful to invariantly transfer information of fields of one type, like mechanics onto the fields of another type like electromagnetism; for example, Helmholtz Hamiltonian mechanics metrics quantifying mechanical fields can be gaged to Coulombic Hilbert metrics, representing Gilbertian and Amperian natures of electromagnetic fields.<sup>6,7,8</sup> Gauge transformations typically between possible gauges tend to form a Lie group, in general referred as symmetry group or the gauge group of the theory; Lie algebra of group generators quantifies a Lie group.<sup>9</sup> Typical gauge transformation in general can be any formal, systematic transformation of the potentials that leaves the fields invariant, although in quantum theory it can be perhaps a bit more subtle than that because of the additional degree of freedom represented by the quantum phase, with application to special unitary group supersymmetric mass terms.<sup>9,10</sup>

Electron-positron pair production from vacuum in oscillating electric double pulses was shown to have time delay between two identical pulses strongly affecting the process by shifting its quantum phases similarly to Ramsey interferometry in atomic physics.<sup>11,12</sup> A properly chosen delay can selectively modify the momentum spectra of produced pairs and significantly enhance even the total production probability, without increasing the applied field energy.<sup>12</sup> If monopoles were isolated in nature, they would be found to undergo similar interactions in the electric field as an electric charge undergoes in a magnetic field. For example, the magnetic field of monopoles and the electric field of charges would exhibit the same behavior, and a moving magnetic monopole would induce a circulating electric field.<sup>13</sup>

It is the application of Iyer Markoulakis general formalism<sup>1</sup> capable of gaging Helmholtz decomposition fields onto Pauli Dirac monopole particle fields<sup>14</sup> that is of concern here to model ansatz quantitatively general formalism at Planck level physics. Section 2 shows construct of a Pauli Dirac Planck circuit matrix field gradient of particle monopole flow loop. Section 2.1 configures application modeling using rules of Iyer Markoulakis Helmholtz Hamiltonian mechanics to evaluate eigenvector field bundle matrix of Pauli Dirac Planck quantum dipole biased monopoles+electron-positron particle gaged field circuit, evaluating string gage metrics; additionally, eigenvector of the dipolar biased monopoles, and electron-positron particles with symmetry operations giving SUSY like field matrix and theoretical evaluation technique for algebra of Coulomb gage are presented. Section 3 proceeds Physical Analysis with Results and Discussions, having Section 3.1 discussing by a brief note knowhow of generalizing mass-charge quantum metrics from general formalism of Iyer Markoulakis<sup>1</sup> and that of charge-fields obtained per Section 2 using proof formalism<sup>4</sup> and physics formalism<sup>5</sup> to define observable measurable gage metrics. Section 3.2 analyses electro-magnetic gage metrics fields via quantum Helmholtz Hamiltonian mechanics formalized originally with theory of Iyer Markoulakis generalization provided,<sup>1</sup> evaluating Coulomb gage out of fundamental proof formalism<sup>4</sup> in terms of pure state's coupling constant quantum density matrix with a function operator quantifying action vortex wave functions and the scalar potential of gradient up energy. In Section 3.3 numerical achievements

with operational mechanism are enumerated progressively with sample computations of the size of Pauli Dirac Planck circuit assembly, the monopole space-time equation primarily deriving size of the astro-observable universe. Section 3.4 discusses scenarios analyzing with graphics the PDP circuit assembly model in detail, having simulation of typical Clifford-like rotations of fermion spins. Section 3.5 summarizes applications of the quantum PDP circuitry highlighting experimental techniques, like spin-ice and spinors Bose Einstein condensates that can verify PDP circuitry assembly model. Section 3.5 discusses future proposed project work with subsequent related paper publications. We envisage application of metamaterial and metasurface antennas with compact dimensions and wide bandwidth and metamaterial and metasurfaces for on-chip antennas applicable in THz integrated circuits,<sup>15-18, 19</sup> Metamaterial and metasurface approaches to suppress the mutual coupling for MIMO and SAR antennas,<sup>20, 21</sup> as well as metamaterial and metasurface-inspired antenna's impedance matching networks for RF-end-circuits.<sup>23</sup>

### Theoretical Results Physics Gaging Formalism

Because of its large magnetic charge, the monopole is strongly coupled to a surrounding cloud of virtual electron-positron pairs.<sup>24</sup> Formation of monopole-particle circuitry is modeled schematically here, called as matrix Pauli Dirac Planck circuit consisting of south monopole S, electron e-, north monopole N, and positron e+. Our present modeling suggests a clocking mechanism may work operating energy generation at the quantum level.

**Schematic of matrix Pauli Dirac Planck circuit**

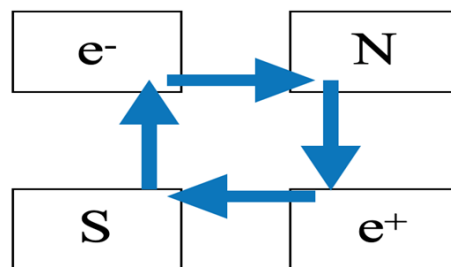


**Fig.1: Schematic modeling Pauli Dirac Planck circuit assembly**

e-: electron; e+: positron particles; N: north, and S: south monopoles – flow of arrow shows gradient vortex matrix circuit.

In the production of typical electron-positron pairs, their natural oscillatory behaviors have been shown to exist;<sup>12</sup> moving magnetic monopole would induce a circulating electric field.<sup>13</sup> Hence in the PDP circuit assembly of electron-positron particles with north south monopoles, oscillations will translate to revolution of the whole assembly, having those oscillations with strong correlations to rotations.<sup>25</sup> This will also induce rotation of the electron-positron plane around north-south magnetic tensor axis; variant exists also having rotation of the north-south plane around electron-south electric tensor axis. We will have to consider also spin of electron-positron particles as well as that of the monopolar quasi-particles to get a complete description of dynamic equation of state of PDP assembly. We will graphically discuss at Section 3 Physical Analysis within this paper the whole aspects with PDP circuit assembly dynamics that are within the scope of this paper. We will have more extensive computer programming simulations validating PDP circuit assembly in our sequential papers.

**Configuring Application Matrix Iyer Markoulakis Helmholtz Hamiltonian Mechanics Monopole Particle Gaged Field Circuit**

Substituting field equivalents of gradient monopole rotational particle Iyer Markoulakis Helmholtz Hamiltonian mechanics theory<sup>1</sup> of algebra for Pauli Dirac Planck circuit matrix, per Figure 1 in Section 2 above, we can get:

$$\begin{pmatrix} \hat{\mathbf{e}}_{r,\mu\nu} & \hat{\mathbf{e}}_g^{\mu\nu} \\ \hat{\mathbf{e}}_{g,\mu\nu} & \hat{\mathbf{e}}_r^{\mu\nu} \end{pmatrix} =::<= \begin{pmatrix} \hat{\mathbf{e}}_{e-} & \hat{\mathbf{e}}_n^{\square} \\ \hat{\mathbf{e}}_s & \hat{\mathbf{e}}_e^+ \end{pmatrix} \dots(1)$$

with  $\hat{\mathbf{e}}_{g,\mu\nu}$ : gradient converging field gaged to  $\hat{\mathbf{e}}_s$ : south monopole field;  $\hat{\mathbf{e}}_{g,\mu\nu}$ : gradient diverging field gaged to north  $\hat{\mathbf{e}}_n^{\square}$  monopole field; similarly,  $\hat{\mathbf{e}}_{r,\mu\nu}$ : rotational vortex converging field gaged to  $\hat{\mathbf{e}}_{e-}$ : electron particle metrics field, and then  $\hat{\mathbf{e}}_r^{\mu\nu}$ : rotational vortex diverging field gaged to  $\hat{\mathbf{e}}_e^+$ : positron particle metrics field; together they are forming field matrix.

Eigenvector calculations performed already in Iyer Markoulakis general formalism<sup>1</sup> are substituted for gage values.  $|\lambda_{dn}>$ : eigenvector of dipolar biased north monopole (having proximity of the north and south monopoles making them act like dipole having bias to the closer monopole); similarly,  $|\lambda_{ds}>$ : eigenvector of dipolar biased south monopole;  $|\lambda_{dn}^*>$  and  $|\lambda_{ds}^*>$

are conjugate eigenvectors of  $|\lambda_{dn}>$  and  $|\lambda_{ds}>$  respectively, while  $|\lambda_{e-}>$  and  $|\lambda_{e+}>$  are eigenvectors of the electron and positron particles, following rules of Iyer Markoulakis general formalism linking them to the appropriate field matrix vectors' quanta, comparing Equations (12)<sup>1</sup> taking care of signs with appropriate substitutions like Equation 35,<sup>1</sup> we derive the following:

$$\begin{aligned} |\lambda_{dn}> &= \begin{pmatrix} -(\hat{\mathbf{e}}_s \hat{\mathbf{e}}_n^{\square})^{0.5} \\ \hat{\mathbf{e}}_n^{\square} \end{pmatrix}; |\lambda_{ds}> = \begin{pmatrix} \hat{\mathbf{e}}_s \\ -(\hat{\mathbf{e}}_e \hat{\mathbf{e}}_n^{\square})^{0.5} \end{pmatrix}; \\ |\lambda_{dn}^*> &= \begin{pmatrix} \hat{\mathbf{e}}_s \\ (\hat{\mathbf{e}}_e \hat{\mathbf{e}}_n^{\square})^{0.5} \end{pmatrix}; |\lambda_{ds}^*> = \begin{pmatrix} (\hat{\mathbf{e}}_s \hat{\mathbf{e}}_n^{\square})^{0.5} \\ \hat{\mathbf{e}}_n^{\square} \end{pmatrix}; \\ |\lambda_{e-}> &= \begin{pmatrix} 1 \\ 0 \end{pmatrix}; |\lambda_{e+}> = \begin{pmatrix} 0 \\ 1 \end{pmatrix} \dots(2) \end{aligned}$$

Here,  $|\lambda_{dn}>$ : eigenvector of dipolar biased north monopole;  $|\lambda_{ds}>$ : eigenvector of dipolar biased south monopole;  $|\lambda_{dn}^*>$  and  $|\lambda_{ds}^*>$  are conjugate eigenvectors of  $|\lambda_{dn}>$  and  $|\lambda_{ds}>$  respectively, while  $|\lambda_{e-}>$  and  $|\lambda_{e+}>$  are eigenvectors of the electron and positron particles;  $\hat{\mathbf{e}}_s$ : south monopole field;  $\hat{\mathbf{e}}_n^{\square}$ : north monopole field.

Equation (1) gives relevant field 2x2 gage matrix, while Equation (2) gives eigenvector fields of these monopole particle circuit components, per Figure 1, specifically characterizing each entity of monopole and particle in detail completely. With this algebra, we can compile matrix assembly with combinatorial eigenvector bundle of the monopole particle circuitry assembly depicted per Figure 1 in Section 2. We denote  $[\lambda_{\text{PauliDiracPlanckcircuitgaging}}]$  as the combined or combinatorial eigenvector bundle matrix of the  $|\lambda_{e-}>$ : electron particle eigenvector,  $|\lambda_{e+}>$ : positron particle eigenvector,  $|\lambda_{dn}^*>$ : dipolar biased north monopole conjugate eigenvector, and then that  $|\lambda_{ds}^*>$ : dipolar biased south monopole conjugate eigenvector, altogether forming 2x2 eigenvector assembly matrix of eigenvector Planck circuit gaging Pauli Dirac particle monopole quantum fields. These are the constructs shown below.

$$[\lambda_{\text{PauliDiracPlanckcircuitgaging}}] = \begin{pmatrix} |\lambda_{e-}> & |\lambda_{dn}^*> \\ |\lambda_{ds}^*> & |\lambda_{e+}> \end{pmatrix} \dots(3)$$

with  $[\lambda_{\text{PauliDiracPlanckcircuitgaging}}]$ : combinatorial eigenvector bundle matrix of the  $|\lambda_{e-}>$ : electron particle eigenvector,  $|\lambda_{e+}>$ : positron particle eigenvector,  $|\lambda_{dn}^*>$ : dipolar biased north monopole conjugate eigenvector, and  $|\lambda_{ds}^*>$ : dipolar biased south monopole conjugate eigenvector.

Substituting these eigenvectors' values from Equation (2) to Equation (3), we arrive thus:

$$[\lambda_{\text{PauliDiracPlanckcircuitgaging}}] = \begin{pmatrix} (1) & ((\hat{\epsilon}_s \hat{\epsilon}_n^{\square})^{0.5}) \\ (\hat{\epsilon}_s) & (\hat{\epsilon}_n^{\square}) \\ ((\hat{\epsilon}_s \hat{\epsilon}_n^{\square})^{0.5}) & (0) \\ (\hat{\epsilon}_n^{\square}) & (1) \end{pmatrix} \dots(4)$$

having  $[\lambda_{\text{PauliDiracPlanckcircuitgaging}}]$ :combinatorial eigenvector bundle matrix;  $\hat{\epsilon}_s$ :south monopole field;  $\hat{\epsilon}_n^{\square}$  north monopole field.

Symmetry operations will lead to collapse of above matrix, because of the zero of  $(1)$  canceling  $\hat{\epsilon}_s$  of

$$\begin{pmatrix} \hat{\epsilon}_s \\ ((\hat{\epsilon}_s \hat{\epsilon}_n^{\square})^{0.5}) \end{pmatrix} \text{and similarly } 0 \text{ of } \begin{pmatrix} 1 \\ (\hat{\epsilon}_n^{\square}) \end{pmatrix} \text{canceling } \hat{\epsilon}_n^{\square} \text{ of}$$

$\begin{pmatrix} ((\hat{\epsilon}_s \hat{\epsilon}_n^{\square})^{0.5}) \\ \hat{\epsilon}_n^{\square} \end{pmatrix}$ , effectively with overlapping elemental metrics field actions. Resultant will give eigenvectorPauli Dirac Planck circuit gaging assembly matrix, per Figure 1, simplified to that below:

$$[\lambda_{\text{PauliDiracPlanckcircuitgaging}}] = \begin{pmatrix} \mathbf{1} & ((\hat{\epsilon}_s \hat{\epsilon}_n^{\square})^{0.5}) \\ ((\hat{\epsilon}_s \hat{\epsilon}_n^{\square})^{0.5}) & \mathbf{1} \end{pmatrix} \dots(5)$$

Here, $[\lambda_{\text{PauliDiracPlanckcircuitgaging}}]$ :combinatorial eigenvector bundle matrix;  $\hat{\epsilon}_s$ : south monopole field;  $\hat{\epsilon}_n^{\square}$  north monopole field.

We can evaluate matrix in Equation (5); cross-diagonals are conjugate elements, same magnitude Hence, determinant $||\lambda_{\text{PauliDiracPlanckcircuitgaging}}|| = ||\lambda_{\text{PDPcg}}|| = 1 - \hat{\epsilon}_s \hat{\epsilon}_n^{\square} \dots(6)$

having  $||\lambda_{\text{PauliDiracPlanckcircuitgaging}}|| = ||\lambda_{\text{PDPcg}}||$ : determinant of the combinatorial eigenvector bundle matrix;  $\hat{\epsilon}$ : south monopole field, and  $\hat{\epsilon}_n^{\square}$  north monopole field.

If  $\hat{\epsilon}_n^{\square} = \hat{\epsilon}_n^{\square}$  and  $\hat{\epsilon}_s = \hat{\epsilon}_s^*$ , then  $||\lambda_{\text{PDPcg}}|| = 1 - \epsilon^2$ , with  $\hat{\epsilon}_n^{\square}$  and  $\hat{\epsilon}_s = \epsilon$ , , having samescalarvalue; this equation otherwise may then be written like quadratic equation form:

$$\epsilon^2 + ||\lambda_{\text{PDPcg}}|| - 1 = 0, \text{ giving that: } \epsilon = +/- (1 - ||\lambda_{\text{PDPcg}}||)^{0.5} \dots(7)$$

with  $\epsilon = \hat{\epsilon}_n^{\square} = \hat{\epsilon}_s$ : same scalar value of  $\hat{\epsilon}_s$ :south monopole field;  $\hat{\epsilon}_n^{\square}$  north monopole field; $||\lambda_{\text{PDPcg}}||$ :determinant of the combinatorial eigenvector bundle matrix.

We can also, in general, write having  $\hat{\epsilon}_n^{\square} = \hat{\epsilon}_n^{\square}$  and  $\hat{\epsilon}_s = \hat{\epsilon}_s^*$ , giving eigenvector matrix:

$$[\lambda_{\text{PauliDiracPlanckcircuitgaging}}] = [\lambda_{\text{PDPcg}}] = \begin{pmatrix} \mathbf{1} & \epsilon \\ \epsilon^* & \mathbf{1} \end{pmatrix} \dots(8)$$

with  $[\lambda_{\text{PauliDiracPlanckcircuitgaging}}]$ :combinatorial eigenvector bundle matrix, to have that,  $\epsilon$ :scalar value of south and north monopole field, and  $\epsilon^*$ : conjugate value of  $\epsilon$ .

Here,  $[\lambda_{\text{PDPcg}}]$  matrix Equation (8) is like SUSY,<sup>26</sup> having Hermitian quantum matrix.<sup>27, 28</sup> With electron-positron annihilation alongside monopoles north and south collapsing to dipolar "stable" magnetism, that is like stringmetrics gage;<sup>5</sup> however, in this case it will be like electromagnetic gaging fields.<sup>6-10</sup>

Recent experiments with John Hodge<sup>29</sup> show that forces of south poles are slightly stronger than the north poles; that will mean in our context  $\hat{\epsilon}_s > \hat{\epsilon}_n^{\square}$  slightly. Therefore,  $[\lambda_{\text{PDPcg}}]$  will have asymmetry metrics, thereby asymmetric\strings\gage\metrics, having non-Hermitian quantum matrix.<sup>30-32</sup> This will point to anisotropic asymmetric eccentric precession with electromagnetic gaging fields.<sup>33</sup> Together with stringmetrics gravity<sup>4</sup> it will then constitute electromagnetic gravity.<sup>34</sup>

**Physical Analysis with Results and Discussions  
Brief Note about Generalizing Mass-Charge and Charge-Fields Gage Metrics to Quantum Relativity Gage Metrics**

Generalizing both gage metrics to get quantum relativity gage unitary metrics will have to undergo overall scheme:

$$\text{mass\charge\gage\quantum\metrics} / \text{Iyer\Markoulakis\general\formalism\metrics} \Rightarrow \text{quantum\relativity\gage\unitary\metrics} / \text{quantum\charge\gage\metrics\fields}$$

This will then involve comparing Pauli Dirac Planck circuit gage, referring Figure 1

$$\text{also:} [\lambda_{\text{PauliDiracPlanckcircuitgaging}}] = \begin{pmatrix} \mathbf{1} & \epsilon \mathbf{dn}^* \\ \epsilon \mathbf{ds}^* & \mathbf{1} \end{pmatrix} [\text{Coulomb Hilbert gage}] = \begin{pmatrix} \hat{M}_{r,\mu\nu}^{\square} & \hat{G}_g^{\mu\nu} \\ \hat{G}_{g,\mu\nu}^{\square} & \hat{M}_r^{\mu\nu} \end{pmatrix} \dots(9)$$

which is Equation (5) in.<sup>5</sup>

[Coulomb Hilbert gage] is essentially the mass\charge\gauge\quantum\metrics, while  $[\lambda_{\text{PauliDiracPlanckcircuitgaging}}]$  is essentially, quantum\charge\gauge\metrics\fields.

having  $[\lambda_{\text{PauliDiracPlanckcircuitgaging}}]$ : combinatorial eigenvector bundle matrix;  $\epsilon_{dn}^*$ : dipolar biased north monopole conjugate field;  $\epsilon_{ds}^*$ : dipolar biased south monopole conjugate field; and the  $\{\hat{G}_{g,\mu\nu}^{\square}, \hat{G}_g^{\mu\nu}\}$  Coulomb gage, having Gilbertian nature with branching to Hilbert gauge down and up rotational vortex fields; also,  $\{\hat{M}_{r,\mu\nu}^{\square}, \hat{M}_r^{\mu\nu}\}$ , having M's like Higgs metrics mass of Higgs-Boson matter, quantifying inertia with gravitational field manifestations, having Amperian nature and conforming to partial differential equations of vortex and the gradient fields obtained per Iyer Markoulakis original formalism.<sup>1</sup>

We will have to examine general formalism with Coulomb Hilbert gage metrics shaping spacetime symmetry alongside Pauli Dirac Planck circuit assembly in Figure 1 revealing typical electromagnetic gage metrics fields, then put them together to get generalism unitary gage quantum\relativity\gage\unitary\metrics. Per physics<sup>5</sup> Coulomb gage,  $\hat{G}_g^{\square}$ , may be algorithmically evaluated having proof mathematical matrix<sup>4</sup> per procedural scheme, showing scalar potential,  $V = \|\nabla^{\square} E_g^{\mu\nu}\|$ , related to gage metrics fields of Pauli Dirac Planck circuit gage.  $\{\epsilon_{dn}^*, \epsilon_{ds}^*\}$  refer to quantum magnetic monopolar cross-diagonal fields, whereas  $\{\hat{G}_{g,\mu\nu}^{\square}, \hat{G}_g^{\mu\nu}\}$  refer to Coulomb quantum gage particle metrics per matrix formulation:  $\hat{G}_g^{\square} = (\langle \Psi_{\mu}(t) | \Psi^{\mu}(t) \rangle)^{-1} \|\nabla^{\square} E_g^{\mu\nu}\| \rho(t)$  of electron-positron cross-diagonal fields. Similarly, “1”s refers to particle diagonal eigenvector fields with Pauli Dirac Planck circuit gage, whereas  $\{\hat{M}_{r,\mu\nu}^{\square}, \hat{M}_r^{\mu\nu}\}$  refer to Hilbert Higgs metrics gage diagonal eigenmatter. Hence non-Hermitian CPT physics will have to consider these aspects while generalizing both gages – matter and fields, having diagonal terms constituting pressure matter gage metrics, cross-diagonal terms constituting electro-magnetic gage metrics fields.

**Electro-Magnetic Gage Metrics Fields Energy Quanta Point Detailing the Working of Pdp Circuit Assembly Effectively**

To consider about electro-magnetic gage metrics fields acting energy on quanta point fields, theoretical

general formalism with Iyer Markoulakis Helmholtz Hamiltonian mechanics quantum field matrix will be applicable exactly.<sup>1</sup> Problem solving with the gage equation:  $\hat{G}_g^{\square} = (\langle \Psi_{\mu}(t) | \Psi^{\mu}(t) \rangle)^{-1} \|\nabla^{\square} E_g^{\mu\nu}\| \rho(t)$ , derived from mathematical physics first principle’s proofing technique<sup>4</sup> have been successfully adapted to physics formalism with Iyer Markoulakis Helmholtz Hamiltonian mechanics transformed to Coulomb gage.<sup>5</sup> In this respect, Iyer Markoulakis theory<sup>1</sup> has specifically concentrated on quantifying Helmholtz decomposition fields analysis of vortex dynamics that have been observed by macro-scale synthetic magnetic monopole assembly experimental technique using Ferrocene.<sup>2</sup> This extensive quantum model ansatz formalism provided eigenvectors, wavefunctions, as well as partial differential equations characterizing zero-point gradient fields and point microblackhole vortex fields that have been then converted to Coulomb gage to equivalently characterize electromagnetic point quanta.<sup>5</sup> In the above equation of the Coulombic gage:  $\hat{G}_g^{\square} = (\langle \Psi_{\mu}(t) | \Psi^{\mu}(t) \rangle)^{-1} \|\nabla^{\square} E_g^{\mu\nu}\| \rho(t)$ , with wavefunctions as a function of time,  $\Psi(t)$ , with upper and the lower indices quantifying down and up vortex fields; gradient up energy,  $\|\nabla^{\square} E_g^{\mu\nu}\| = V$ , the scalar potential; and  $\rho(t) =$  quantum density matrix, typically representing pure state’s like coupling constant in general relativity;<sup>35</sup> overall we may also define a function operator,  $f$  quantifying  $(\langle \Psi_{\mu}(t) | \Psi^{\mu}(t) \rangle)^{-1} \|\nabla^{\square} E_g^{\mu\nu}\|$  considered as transforming micro to macro parametrically  $\rho(t)$  to  $\hat{G}_g^{\square}$ . Together they all fully define the gage metrics quantifiable observable measurement physics.<sup>4, 5</sup>

Limitations of PDP circuit model are that we do not know exactly particular interactive features of the circuit oscillator. It is too complicated that only after simulation programmatically verification of oscillator theoretically as well as experimentally its behavior is possible to have a thorough validation overcoming falsifiability aspects. Presently, this aspect project will be undertaken to analyze by Hamiltonian algebra energy geometry algorithm that will launch computer programming simulation projects. We estimate such efforts to be spanning over many months, with subsequent publications of results verifying to validate theoretically as well as with collaborative experimental measurements, discussed briefly in Section 3.5.

We will, however, briefly underscore partial validation of PDP assembly working principle from literature of electromagnetic systems antenna devices that are activated by interactive electrical and magnetic tensor quantum fields.<sup>13, 15-19, 21-23, 25, 36</sup> Eventually, these systems can be quantifiably quantum modeled by applying theoretically developed PDP circuitry assembly, per Figure 1 Section 2 above. Tuning of the antenna may have operational quantum mechanism as per magnetic or electric tensor sticking out and resonating with electromagnetic environment, thus absorbing signal after creating higher signal/noise ratio with resonance effect of the antenna interacting with the environment.<sup>37, 22</sup> If it is that electric or magnetic flux line has dependence on the surface, then a particular electric or magnetic tensor or vector sticks out. One may simplify looking at these phenomena like the character of the surface normal to be either electric in nature or magnetic in nature, that may show observable output in polarization terms.<sup>38</sup> Magnetic tensors have precessing property like the Bohr magneton, whereas electric tensors have more of a translational property in that they move towards each other, like electrons and positrons or protons; water molecules with molecular chemistry coagulates coming together to form structures extending to large macro-spaces with bonds that have charge properties.<sup>40, 41</sup> Whereas the microwave heating property, for example of water is linked to magnetic tensor precessing within the proton and oxygen ion bond symmetry, amongst

other aspects.<sup>39</sup> Electricity and magnetism maybe no separate phenomena but entangled into one we call electromagnetism, and which is expressed with its two interchangeable forces, electric and magnetic as described by Maxwell electromagnetic classical theory.<sup>1-5</sup>

**Graphical Scenarios Analysis with PDP Circuit Assembly**

We will examine the workings of the PDP assembly graphically in scenarios to decipher permutational nature with clocking mechanism that we envisage will be background operational process. Figure 1 when rotated by  $\pi/2$ , i.e.,  $90^\circ$  will have electric tensor sticking out of surface plane of PDP assembly, shown per I and II scenarios of Figure 2. Variation of that will be magnetic tensor sticking out of surface plane of PDP assembly, shown per scenario III of the Figure 2. [VI.1] and [VI.2] in Figure 2 are the results of Section 3.1 above, and the corresponding wave vector,  $k$  value. Figure 3 shows what will happen if two assemblies have electric tensor antiparallel, such that there will be electron-positron attraction and north monopole of one assembly versus north monopole of the adjacent assembly repulsions, for example. Figure 4 shows variational scenario of Figure 3, of what will happen if two assemblies have magnetic tensors antiparallel, such that there will be north-south monopolar magnetic attraction and then, for example, positron of one assembly versus the positron of adjacent assembly repulsions.

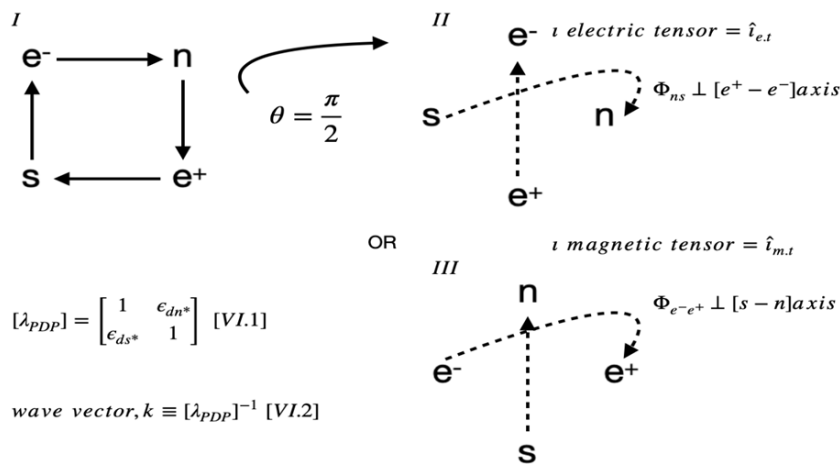


**Fig. 2: Possibilities with (I), (II), and (III) show PDP assemblies' different configurations; [IV-1] and [IV-2] indicate associated matrices, and the wave vector. Here,  $\theta$ : angle of revolving PDP assembly;  $\Phi$ 's: angle of rotating monopole or particle around that electric or magnetic tensor axis;  $\gamma$ : angle of spin associating with each particle or monopole {not shown above now}**

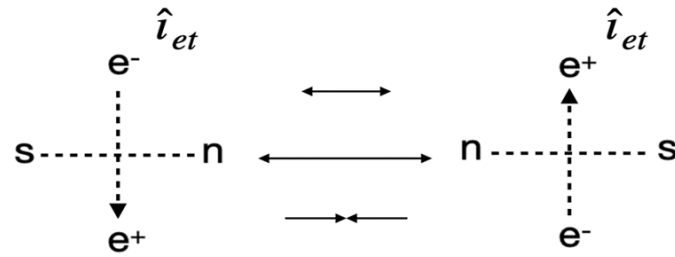


**Fig. 3: Attractive fusing process assemblies, with antiparallel  $\hat{i}_{et}$ : electric tensors sticking out of space-time surfaces of adjacent assemblies, having repulsive north monopoles**

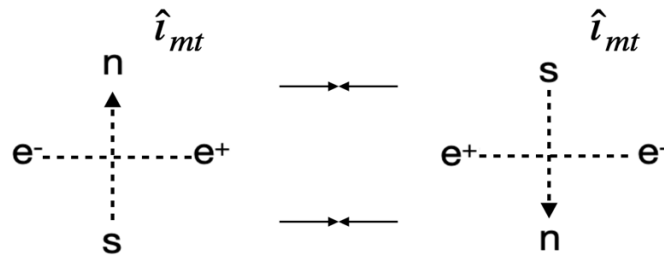


**Fig. 4: Attractive fusing process assemblies, with antiparallel  $\hat{i}_{mt}$ : magnetic tensors sticking out of space-time surfaces of adjacent assemblies, having repulsive positrons**

Figures 5 and 6 depict scenarios when flipped cases of Figures 3 and 4, whereby the electric tensors are in parallel, hence repelling while north monopole versus south monopole of adjacent assemblies have

attractive outcome (Figure 5). Similarly, magnetic tensors are in parallel repelling, while positron versus electron of adjacent assemblies have attractive outcome (Figure 6).

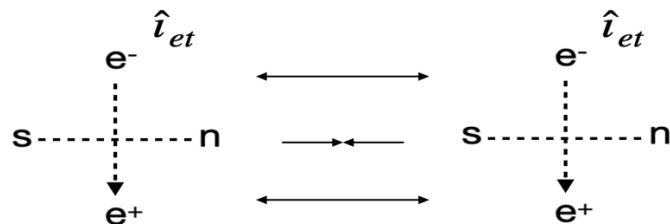


**Fig. 5: Repulsive process assemblies, with parallel  $\hat{i}_{et}$ : electric tensors sticking out of the space-time surfaces of adjacent assemblies, having attractive north-south monopoles**

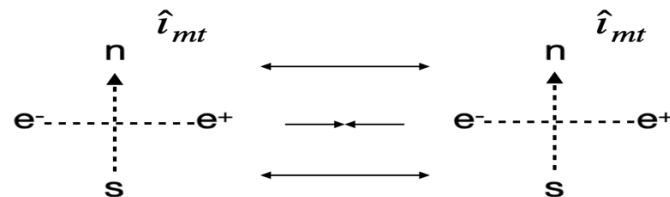


**Fig. 6: Repulsive process assemblies, with parallel  $\hat{i}_{mt}$ : magnetic tensors sticking out of the space-time surfaces of adjacent assemblies, having attractive electron-positron particles**

We analyze graphically in Figure 7 further scenario shown per Figure 3 to see bending of fields space-

time with electron-positron annihilating, then released energy forming neutrino particles, while

north monopoles of adjacent assemblies repelling and forming dipole magnetism away from electric tensors, configuring within spatial fields. Figure 8 graphically analyzes the Figure 4 scenario to see bending of fields space-time with north-south

monopoles of adjacent assemblies forming dipolar magnetism, while positron-positron repulsions of adjacent assemblies pushing electron-positron pairs away from magnetic tensors to cause annihilation released energy forming thereby neutrino particles.

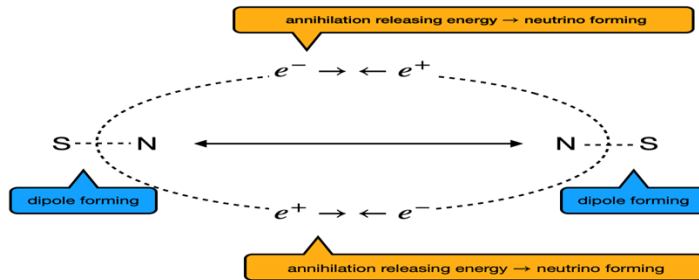


**Fig. 7:** Analysis graphically of scenario shown per Figure 3 schematically showing possible bending of space-time field forming neutrino particles with released energies of annihilated  $e^-$  and  $e^+$ , while north monopoles of adjacent assemblies repelling and forming dipole magnetism away from electric tensors, configuring within spatial fields

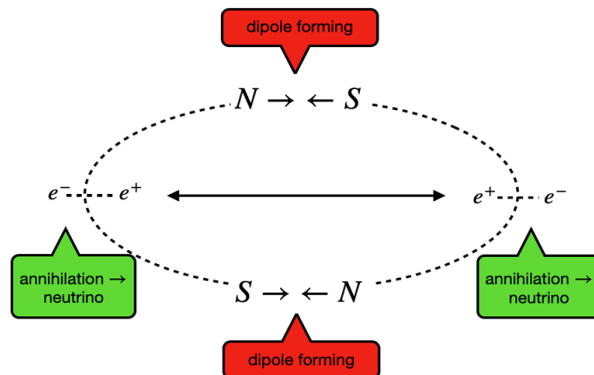


**Fig. 8:** Analysis graphically of scenario shown per Figure 4 schematically showing possible bending of quantum field having north-south monopoles of adjacent assemblies' dipolar magnetism, with positron-positron repulsions of adjacent assemblies pushing electron-positron pairs, annihilation released energy forming neutrino particles, away from the dipoles

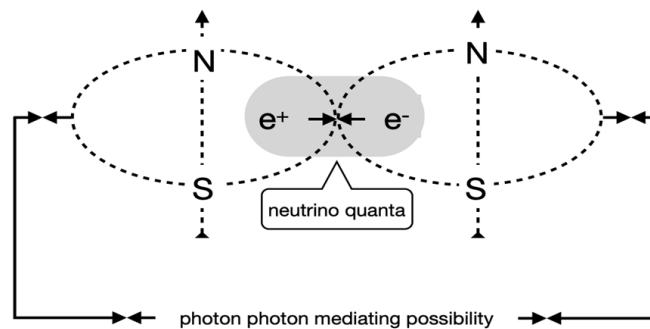


**Fig. 9:** Stabilizing with photonic mediation, with electromagnetism configuring within spatial fields of electric field and magnetic field mutually interacting to origin of particle cell quanta; here, analysis per Figure 6 scenario continued to show space fields with neutrino quanta as well

Analyzing graphically with scenario per Figure 6 in Figure 9 to see bending of fields space-time with electron-positron annihilating then released energy forming neutrino particles, while magnetic tensors of adjacent assemblies repelling. Stabilizing with photon formation with electromagnetism configuring within spatial fields of electric field and magnetic field mutually interacting will lead to an origin of

particle cell quanta. Figure 10 graphically analyzes the Figure 5 scenario to see bending of fields space-time with north-south monopoles of adjacent assemblies forming dipolar magnetism, while parallel electric fields' repulsions of adjacent assemblies pushing them away from dipole magnetism to cause compression of quantum space-time surfaces overall.

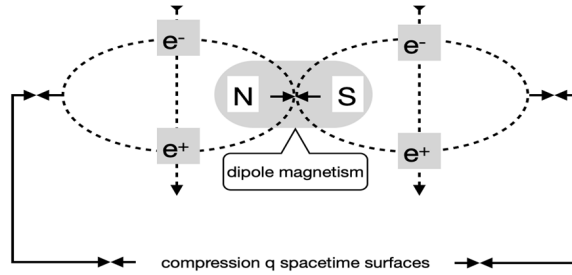


**Fig. 10: Space-time surfaces getting compressed quantum with dipole magnetism forming, per Figure 5 scenario, continued to show electric tensors keeping the space fields quanta as well**

The Clifford-like rotations provides a simple way to model fermion particle spins. We are showing typical example simulating Clifford-like rotations of a typical fermion particle in a geometrical Cartesian xyz coordinate system.

spin of the same fermion particle has been shown after a half-turn, i.e., 90° simulations. The particle takes a full 720° rotation to return to its original state, as expected. These simulations have correlations to verify scenarios partially. Further computer simulations with programming algorithms generated out of Hamiltonian algebra pairing with Clifford algebraic geometry are in the works.

Figure 11 shows spin of fermion particle after one full rotation, while Figure 1b, while in the Figure 12

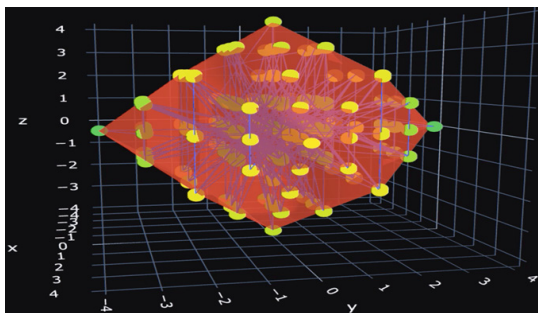


**Fig. 11: Spin of fermion particle after one full rotation**

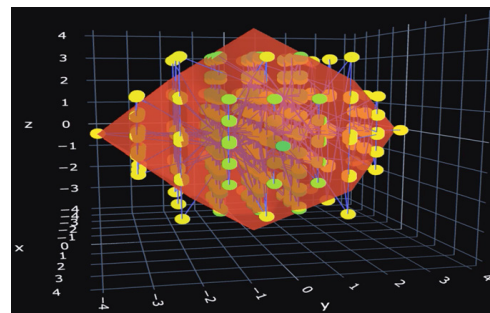


**Fig. 12: Spin of the same fermion particle after a half-turn, i.e., 90°**

**Numerical Achievements With Operational Mechanism with Related Table and Earlier Graphs**  
 Typical numerical values with Iyer Markoulakis general formalism theory paper and problem solving vacuum quanta fields<sup>1, 3</sup> gives zero-point gradient energy, Eg, as per numerical  $[(2-i\hbar)/i\hbar] \approx 10^{26}$  metric unit energy value order of magnitude, and quasi-particles having sizes, with value of  $10^{-26} \text{ m}^3$  (this value after correction to algebraic equation

(8.5) in,<sup>3</sup> erratum sent to journal already) or even less, generated especially by microblackhole compressing monopole mass to  $10^{-11} \text{ kg}$ ; after propagation of these quasi-particles, radius sizes expand to higher values, having reduced monopole mass, closer to  $10^{-47} \text{ kg}$  per equation in attractive-repulsive force fields of entity size,  $r_e \approx 10^{-32} / (Mm)^{1/2}$  meter (this corrected algebraic equation (8.5) in,<sup>3</sup> already erratum sent to the journal)), especially

due to microblackhole mechanism compressing monopole mass from  $10^{-47}$  kg to  $10^{-11}$  kg, with entities propagating away from microblackhole, monopole mass value reducing closer to  $10^{-47}$  kg with evolution of time, continuous propagation of generators assisted by quantum field photon mediators will be expected to create quarks, antiquarks, as well as gluons out of vacuum quanta,<sup>3</sup> and the universe size estimated by Iyer Markoulakis general problem solving theoretical analysis providing a value of observable universe, briefly shown within derivation essentially below. We estimate the size of Iyer Markoulakis Helmholtz Hamiltonian mechanics Pauli Dirac Planck monopole particle gaged matrix field circuitry assembly in Figure 1 Section 2to be greater than Planck magnitude of  $10^{-34}$  unit and less than quasi-particle size  $10^{-26}$  metrics unit since this circuitry compressed having microblackhole acting.<sup>1-5</sup> We will look further into mathematical as well as physical aspects with our upcoming papers.

Using equations<sup>42-57</sup> relating  $i\Psi$  to  $E/(mc^2)$  (where in general energy, E is different from relativistic particle matter energy,  $mc^2$ ), and  $E_o/E_g \cong kr^2/ke$  equation (8.1),<sup>3</sup> where  $E_o$  is the vacuum energy and  $E_g$  is the zero-point gradient energy, we may write  $E_o/E_g = f(r)$ , where k and  $k_g$  are constants. We can show that  $\frac{\partial}{\partial t} [f(r)] = f'(r) \cdot v = \frac{\partial}{\partial t} (E_o/E_g) = 10E_o/E_g \cdot \frac{\partial}{\partial t} (M_m r^2) = 10^{18} \cdot \frac{\partial}{\partial t} (M_m r^2) = 10^{18} M_m \cdot 2r \cdot v$ , if  $M_m \neq f(t)$ , having  $v = \frac{\partial}{\partial t} (r)$ , r is the radial distance from zero-point, using equations (8.1) & (8.3).<sup>3</sup> Simplifying, noting that  $E/(mc^2)$ <sup>57</sup> can be written as a function of r, we can get equations  $f(r) = E/(mc^2) \cong 10^{18} M_m \cdot \int_t r \cdot dt$ . Equating  $i\Psi$  to  $E/(mc^2)$ ,<sup>57</sup> we can equate therefore:  $i\Psi \cong 10^{18} M_m \cdot \int_t r \cdot dt$ . For the

PDPcg, per schematic within the section 2 above, if we have  $\Psi = \Psi_{NSZP}$  where NSZP is a north south zero point dipole/monopole magnetic “quagmire” having imaginary value “i”, then from above:  $i\Psi = i \cdot i = -1 \cong 10^{18} M_m \cdot \int_t r \cdot dt$ . Thereby, we will obtain the value of  $\int_t r \cdot dt \cong -10^{-18} (M_m)^{-1}$ . We mentioned above that monopole mass can vary from  $10^{-47}$  kg to  $10^{-11}$  kg. In the region of a microblackhole,  $M_m = 10^{-11}$  kg, and hence in magnitude  $\int_t r \cdot dt \cong 10^{-8}$  space-time unit metrics or a little higher value corresponding to size of a hydrogen atom. However in a zero-point far away from microblackhole,  $M_m = 10^{-47}$  kg and hence  $\int_t r \cdot dt \cong 10^{28}$  space-time unit metrics or a little higher value in magnitude, corresponding to observable size of universe!! These calculations have already demonstrated the power of the Iyer Markoulakis general formalism problem solving results that shows real correlation to physical observables’ measures. We will also investigate how relativistic astrophysical general metrics affect the observables; astrophysical equations, modifying on Einstein-Maxwell spacetime fields equations evaluating these metrics will be extensively considered as continuing articles of the present paper. Charge of a monopole is  $1/2e$ , and the monopole core size is  $10^{-28}$  cm<sup>24</sup> or  $10^{-30}$  m. Compared to Higgs boson having a lifetime of about  $10^{-22}$  s, a magnetic monopole, if it exists may be absolute stable and can get destroyed only if it contacts with another monopole of having opposite charge.<sup>42</sup> Hence, monopoles may be quasi-particles, coexisting with electron-positron particles, validating the PDP circuitry depicted per Figure 1 in Section 2 above.

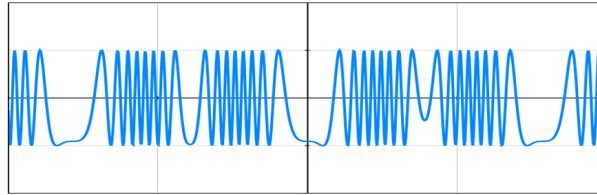
**Table 1: Summary with data of numerical achievements with operational mechanism**

Property	Unit Measuring	Source reference	Numerical value range
Monopole mass, M	Kilogram, kg	24	$10^{-47}$ to $10^{-11}$
Monopole core size	Meter, m	24	$10^{-30}$
Monopole charge	Electron unit	24	$1/2e$
Fermion size	Meter, m	43, 44	$10^{-18}$ to $10^{-15}$
Zero-point gradient energy, Eg	Metric unit	1, 3	$10^{26}$
Zero-point microblackhole entity size	Meter, m	3	$10^{-8}$ to $10^{-26}$
Space-time extent, macro to micro	Metric unit	Derived estimation	$10^{28}$ to $10^{-8}$
PDP circuitry size	Meter, m	Derived estimation	$<10^{-26}$

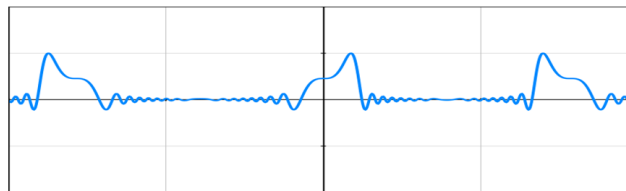
Table I below summarizes numerical achievements with operational mechanism that are applicable

for ongoing analytical modeling experimental parameters practically discussed above.

We are also presenting graphs relating to action of point gradient and action vortex fields,<sup>3</sup> providing a key graphical input in modeling and subsequent programming simulations.



**Graph I: showing vortex generating sinusoidal pulsed signal output. Input X: function vortex; Y: sinusoidal (function of X) having output signals, with input per theoretical analyses modeling<sup>1,3</sup> that will indicate signals asymmetrical due to combined fields, per Hamiltonian algebra<sup>1,3</sup>**



**Graph II: Analytically graphing the value of “r” & distribution profile of typical equivalent wave velocity in vacuum space vortex quanta, using values of the electric constant =  $8.85418782 \times 10^{-12} \text{ m}^{-3} \text{ kg}^{-1} \text{ s}^4 \text{ A}^2$ , and magnetic constant =  $1.25663706 \times 10^{-6} \text{ m kg s}^{-2} \text{ A}^{-2}$ , applied to the Graph I signal spectra, per Hamiltonian algebra<sup>1,3</sup>**

#### **Applications Of the Quantum Pdp Circuitry Highlighting Experimental Techniques Validating Pdp Circuitry Model**

Once quantum PDP circuitry can be verified by experimental techniques, then it will have many wide-ranging applications like the quantum computers, quantum supercomputing expertise supercomputing networks, alongside quantum astrophysical grand unifying genesis physical electromagnetic gravitational matter antimatter systems.

Continuing with Section 3.4 advantages having numerical achievements correlating with state-of-the-art literature, Graph I and Graph II alongside Figures 1 through 12 indicate typical periodicity observables that are reminiscent of time crystals made of electron-positron pairs.<sup>45</sup> Also, supporting literature are electron-positron pair, also known as positronium creation with crystal photons.<sup>46</sup> Using Ferrolens,<sup>1</sup> physical observations of macroscopic prototype synthetic magnetic unipole array show unambiguously exhibiting magnetic monopole behavior, successfully emulating Dirac magnetic monopoles.<sup>47</sup> We can state only knowhow that electric and magnetic tensors can interact with

antenna electromagnetic quantum fields; this PDP circuit potentially can overcome quantum computing problem of interference from environment<sup>48</sup> and perform data retrieval information feasibly out of the circuit.<sup>49</sup> We will have extensive usage of data from Table I, Graph I, and the Graph II, alongside Figures 1 to 12, incorporating Clifford Algebra to compute rotational mechanics with PDP assembly in our related papers that are upcoming.

With regards experimental projects, monopole observations measurements applying gap length gage equation of motion trajectory relativistic tracking while separately measuring change of the monopoles' masses temporally, utilizing spin-ice techniques<sup>50</sup> as well as measurements of spinors Bose-Einstein observable condensates, demonstrating curved space Klein-Gordon equations with Mexican hat scalar field potential<sup>51</sup> will reveal worldline, timeline event, and space time matter antimatter characterizations. Separately measuring object trajectory and mass with independent verifications having spin-ice and Bose-Einstein condensate measurements will overcome Heisenberg uncertainty measurement problem with the falsifiability results.

We may explain double slit's experiment from the PDP circuitry, based on the clocking angle ( $\theta$ ), angle of revolving PDP assembly; ( $\Phi$ 's), angle of rotating monopole or particle around PDP assembly's electric or magnetic tensor axis; ( $\gamma$ ) angle of spin associating with each particle or monopole and spin. Spin wavefunction of the observer versus object is what will matter and then how it collapses to get observable observations. Additionally, Clifford algebra will be incorporated to take care of 4D space-time quaternion rotations.

### Future Work Project and Subsequent Paper Publications

Finite element modeling with individual circuitry grids forming the element, and the electric magnetic tensors forming nodes provide numerical quantifiable simulation network modeling to evaluate application of PDP circuitry assembly in Figure 1 with scenarios Figures 2 to 10 and simulations of rotations Figures 11 and 12 to obtain electroweak operational fields and the strong-nuclear fields, depending on the node that is sticking out of the space-time entity-environment element interface. Then we will be quantifiably simulating real electromagnetic actions like in antenna devices. This is vast research and computing project, that is out of the scope of the present paper; however, that is a good start for upcoming papers to delve into more numerical outputs obtainable out of a finite element modeling with program simulation capabilities with a visual graphic animation. Figure 10 with Section 3.3 above will likely be the best scenario for a finite element modeling analysis with having computer programming followed by simulation theoretical validation. Electric tensors of adjacent assemblies, per Figure 10 with Section 3.3 above, can act as cells – elements, while dipole magnetism as nodes of such F.E.M. program. One evaluator will be compression of quantum space-time surfaces, one of the predictors from theoretical analysis with PDP model. We will proceed to computer programming with Hamiltonian algebra energy geometry providing algorithm to simulate quanta energy with relativistic fields stabilization of quasi-particles to particles to photon phonon real universe.

To understand structural geometry formed from vacuum quanta out of point fields' quantitative theory,<sup>1, 5</sup> it is presently required to grapple symmetry, structure, and formation of real space

with knowledge of symmetry inherently naturally originating with mechanism characteristics also permutating fundamental processes of prime numbers' factorization. We will examine this extensively in subsequent papers. Physics formalism paper<sup>5</sup> brings out aspects with importance of diagonal terms of the gage matrix showing Hilbert Higgs metrics  $0 \rightarrow \mathbf{M}$ , signifying action to matter inertia effectively operating with gravitational field moving from vacuum to matter,  $\mathbf{M}$ . In general, that will represent characterization of Helmholtz transformation symplectics to Higgs field, having subsequent Higgs mechanism to originate God particle giving flavor mass particle Higgs Boson system.<sup>52</sup>

Vacuum quanta may have only random scatter points patterns with fabric of the space,<sup>1, 5</sup> in primordial universe. Research extensively performed about magic square symmetry and how that may represent natural mechanisms with which point patterns align to form crystals have been explored quite recently, especially with Christopher O'Neill's simulations to study, for example, the typical patterns of the 48 particles of the DGO Standard Model assigned vertices in the 288-cell, as part of Quantum Physics project with Magic Squares, the Weak Force, and the Higgs Mechanism.<sup>53</sup> It should be possible to unify the 48 S (8) Matrices of the DGO Standard Model with the Iyer Markoulakis Helmholtz Hamiltonian mechanics<sup>1</sup> with the presented model, Figure 1 in Section 2 above of monopole particle PDP gaged field circuitry assembly.

Additionally, Iyer's physics conjecture with recent quantum modeling articles<sup>1, 3, 4, 5</sup> lead to proposition that prime numbers' factorization of these random pop-up particles within vacuum<sup>1, 54</sup> will be a natural operational mechanism. Basis of that is seen in the symmetrical universal map with Hubble Space Telescope, theoretically corresponding to the Emmy Noether's theorem of symmetry principle, discussed elsewhere;<sup>1</sup> these can provide us an intuition that there may be inherent quantum asymmetry and there is driving force to attain symmetrical universe. However, only matter particle arrangements within the typical form of magic square symmetries are possible and that rotations/revolutions of matter are necessary to have group symmetry, also that in the process of which it will have to fractionate to fractal elements. Hence the scatter distributions

of constellations, galaxies, stars, planets, and satellites make sense thereby, with also periodic lattice arrangement of atoms, five-fold symmetry with micro-crystals, as well as macro-crystal symmetry, with even supersymmetry<sup>6, 27</sup> Quite detailed study about magic squares group symmetries revealing natural mechanisms operating will be revealed by articles continuing with this paper. We will strive to achieve understanding with knowledge of magic square symmetry mathematical physics revealing symmetry, structure, and formation of a natural operational real space geometry.

To consider about pressure matter gage metrics, shaping sense time space symmetry, aspects will have to be quantified applying relativistic Einstein metric of the Minkowski space time equation systems:  $ds^2 = -dt^2 + dx^2 + dy^2 + dz^2$  in Cartesian coordinates; in spherical coordinates, it is  $ds^2 = -dt^2 + dr^2 + r^2 d\theta^2 + r^2 \sin^2\theta d\phi^2$ .<sup>55</sup>

Rewriting in the vacuum continuum form in general metric form conjectured here:

$$df^2 = ds^2 - g_{1x}dx^2 - g_{1y}dy^2 - g_{1z}dz^2 + g_{1t}dt^2 \quad \dots(10)$$

having  $df^2 =$  modified Einstein-Minkowski space time metric with sense, the difference of relativistic Einstein-Minkowski metric space time,  $ds^2$  equation in system Cartesian coordinates  $(x, y, z, t)$ ;  $\{g_{1x}, g_{1y}, g_{1z}, g_{1t}\}$  relativistic general metrics, corresponding to each of the coordinates  $(x, y, z, t)$ .

Equation (10) having  $\{g_{1x}, g_{1y}, g_{1z}, g_{1t}\}$  relativistic general metrics thus will account for curving or shaping of the  $[x, y, z, t]$  spacetime topology, generalizing modification of functional parametric symmetric factor,  $df^2 = 0$  which will correspond to vacuum solution with zero sense, if we have a five-dimensional sense time space universe, while vacuum monopoles probably occur infinitely with having universal vacuum quanta cosmos extent.<sup>56, 57</sup> There are many astrophysical equations, modifying on Einstein-Maxwell spacetime fields equations to evaluate these metrics, like of which astrophysics that Manuel Malaver have investigated extensively;<sup>58</sup> we will be exploring in later publication a unification of quanta energy with astrophysical relativistic fields.

Modeling of a dark energy Star's theory based on Einstein-Gauss-Bonnet gravity equations has

highlighted critical aspects of space time metrics.<sup>58</sup> Our goal will be to achieve general derivation having the sense-time-space metrics within Equation (10) having in there  $\{g_{1x}, g_{1y}, g_{1z}, g_{1t}\}$  relativistic space time general metrics, that will be shaped or curved also according to Iyer Markoulakis quantum formalism and magic squares group symmetries. Thus, we will obtain quantitative means to account for curving or shaping of the  $[x, y, z, t]$  spacetime topology, generalizing modifying parametric symmetric factor, with the function  $df^2$  corresponding to typical sense solution of a five-dimensional sense time space universe.<sup>56-58</sup> These astrophysical equations, modifying on Einstein-Maxwell spacetime fields equations evaluating these metrics will be extensively considered as continuing articles following the present paper.

#### Addressing Limitations

The principles of quantum mechanics allow for a substantial improvement on the speed of sets of calculations. For example, quantum computers will theoretically outstrip a traditional computer when trying to factorize large numbers and other intractable permutational or combinatorial problems.<sup>59-62</sup> However, difficulties and limitations arise when attempting to shield such delicate systems from the environment; the common approach is to cool the systems down to close to zero degrees Kelvin.<sup>61, 62</sup> This can be impractical and expensive. Quasiparticles, like the Fibonacci anyons and braiding techniques have been proposed as a solution,<sup>61</sup> since quasiparticles in general are much larger and are less impacted by decoherence from the environment. The PDP circuit offers a similar solution. At present, spin ices can operate at temperatures that are a few degrees above absolute zero.<sup>62</sup> The circuit also benefits from using magnetons, which are quasiparticles on the order of  $10^{-26}m^{-1-3}$  and is the size of the PDP circuit assembly itself [Table I]. The higher temperatures and relatively larger size of the circuit potentially provides a more stable circuit than traditional elementary particle usage, although by how much is unclear.

Another limitation that can arise in both quantum and chemical computing circuits is how to get the information into and out of a system.<sup>63</sup> The PDP circuit interacts directly with an electromagnetic field, which allows the assembly to rotate and to change its state. This state change is crucial to how

the circuit operates and will form the basis of logic gates which will be used to build quantum ternary full adders, multipliers and subtractors. It is assumed that magnetons have been measured inside Spin Ice crystals, but this observation has yet to be confirmed and the particles remain theoretical for this reason. Until such times as the observation is confirmed and the state and position of a single magneton is adequately manipulated by experimentalist in the laboratory, the PDP-circuit and any of its proposed advantages will remain out of reach. The current method for interaction with the theoretical magnetons is to wind a coil around the Spin Ice crystal.<sup>64</sup> Such techniques while successful for recording system wide state changes in the crystal are insufficient for our purposes. In our case, it will likely be necessary to construct narrow channels of spin-ice material (most likely Dy<sub>2</sub>Ti<sub>2</sub>O<sub>7</sub> (dysprosium titanate)<sup>65</sup> embedded in other non-magnetically conductive material, which will then feed out to a traditional mainframe computer via contacts on the surface of the crystal. Obviously, the construction of the circuit could provide other unforeseen limitations in the materials themselves, but what these are is unknown presently to the authors.

**Summary Conclusions**

We have presented configuration of Pauli Dirac Planck circuit assembly gage (PDPcag) that maybe operating at the quantum level, typically consistent with application of point fields matrix theoretical quantum general formalism of Iyer Markoulakis Helmholtz Hamiltonian mechanics with transformed metrics to Coulomb gage. Eigenvector calculations gave gage values of those eigenvectors of dipolar biased monopoles, as well as that of electron and positron particles, alongside their conjugate eigenvectors of appropriate field matrix vectors quanta. We have quantified combinatorial eigenvector bundle of the monopole particle circuit matrix constructs assembly, simplifying with symmetry operations to matrix collapsing resultant eigenvector of

$\begin{pmatrix} \mathbf{1} & (\hat{\epsilon}_s \hat{\epsilon}_n^{int})^{0.5} \\ (\hat{\epsilon}_s \hat{\epsilon}_n^{int})^{*0.5} & \mathbf{1} \end{pmatrix}$ . Evaluation of this monopole-particle fields' matrix provided eigenvector matrix results like SUSY  $\begin{pmatrix} \mathbf{1} & \xi \\ \xi^* & \mathbf{1} \end{pmatrix}$ , having Hermitian quantum matrix representing electromagnetic gaging fields.

Modifying this matrix with experimental observations of John Hodge with magnetic fields' measurements of macro-magnet-poles, eigenvector bundle has been conjectured to have asymmetric strings\gage\ metrics.

Physical Analysis with graphics per Figures 1 to 10 at length discussing scenarios specifically of electric tensor particles and magnetic tensor monopoles permutationally interacting, that provide partial validation, verifying working model of PDP circuit assembly prototyping details. Figures 11 and 12 partially validate the spin aspects with Clifford algebra geometry. Table I shows numerical achievements that include estimated size of PDP assembly. 2 graphs explain vortex generating sinusoidal pulsed signal output distribution profile of typical equivalent wave velocity of the related point fields that will form the mechanism working of PDP circuit analysis, with initial process operating at the quantum level. We have tabulated estimated size of Pauli Dirac Planck circuitry assembly to be greater than 10<sup>-34</sup> Planck magnitude and less than quasi-particle size 10<sup>-26</sup> metrics unit.

We envisage many wide-ranging applications of PDP circuitry assembly quantum model to quantum supercomputing expertise networks, alongside quantum astrophysical grand unifying genesis physical electromagnetic gravitational matter antimatter systems. This will provide project thrust ongoing with Hamiltonian algebra energy geometry algorithm launch computer programming simulations, that we are undertaking to publish results within a few months.

**Acknowledgements**

Encouragements with group projects support of Emmanouil Markoulakis of Hellenic Mediterranean University in Greece, Manuel Malaver of Maritime University of the Caribbean in Venezuela, collaboration efforts communication with Christopher O'Neill of Cataphysics Group Ireland, and perpetual project support of Rajan Iyer with Engineering Inc International Operational Teknet Earth Global Platform collaborations are appreciated highly. Authors acknowledge active stimulating brainstorming discussions@RESEARCHGATE scienceforum.

**Funding**

There is no funding or financial support for this research work.

**Conflict of Interest**

The authors declare no conflict of interest, financial or otherwise.

**References**

- Iyer R., Markoulakis E., Theory of a superluminous vacuum quanta as the fabric of Space, *Physics & Astronomy International Journal*, 5(2), 43-53, (2021).
- Markoulakis E., Konstantaras A., Chatzakis J., Iyer R., Antonidakis E., Real time observation of a stationary magneton, *Results in Physics*, 15, 102793, (2019).
- Iyer R., Problem Solving Vacuum Quanta Fields, *International Journal of Research and Reviews in Applied Sciences*, 47(1), 15-25, (2021).
- Iyer R., Malaver M., Proof Formalism General Quantum Density Commutator Matrix Physics, *Physical Sciences & Biophysics Journal*, 5(2), 000185, (2021).
- Iyer R., Physics Formalism Helmholtz Matrix to Coulomb Gauge, publication in Physical Sciences Forum, Preprints 2021070451, DOI: 10.20944/preprints202107.0451.v1, (2021).
- Cremonesi S., Hanany A., Mekareeyab N., Zaffaroni A., Coulomb branch Hilbert series and Hall-Littlewood polynomials, *Journal of High Energy Physics*, 2014, 0-40, (2014).
- McDonald K., The Helmholtz Decomposition and the Coulomb Gauge, Joseph Henry Laboratories, Princeton University, Princeton, NJ 08544, April 17, 2008, updated March 3, 2020, <https://physics.princeton.edu/~mcdonald/examples/helmholtz.pdf>, (2020).
- Arias-Tamargo G., Bourget A., Pini A., Rodríguez-Gómez D., Discrete gauge theories of charge conjugation, *Nuclear Physics B*, 946, 114721, (2019).
- Randall L., New Mechanisms of Gauge-Mediated Supersymmetry Breaking, *High Energy Physics, Nuclear Physics – Phenomenology Theory*, Section B, 495(1), 37-56, (1997).
- Guendelman E., Douglas Singleton D., Scalar gauge fields, *Journal of High Energy Physics*, 1405, (2014).
- Ehlotzky F., Krajewska K., Kamiński J. Z., Fundamental processes of quantum electrodynamics in laser fields of relativistic power, *Reports on Progress in Physics*, 72, (2009).
- Ruffini R., Vereshchagin G., Xue S. S., Electron-positron pairs in physics and astrophysics: from heavy nuclei to black holes, *Physics Reports*, 487(1-4), 1-140, (2010).
- Di-Piazza A., Müller C., Hatsagortsyan K. Z., Keitel C.H., Extremely high-intensity laser interactions with fundamental quantum systems, *Reviews of Modern Physics*, 84(3), 1177-1228, (2012).
- Granz I. F., Mathiak O., Villalba-Chávez S., Müller C., Electron-positron pair production in oscillating electric fields with double-pulse structure, *Physics Letters B*, 793, 85-89, (2019).
- Sravanth C., Chattopadhyay A., and 13 others contributed, Magnetic Field Lines, BRILLIANT, <https://brilliant.org/wiki/magnetic-field-lines>.
- Bollini C. G., Ferreira P. L., On the Motion of a Charged Particle in the Field of a Magnetic Monopole, *Nuclear Physics B*, 137(3), 351-358 (1978).
- Alibakhshikenari M., Virdee B. S., Ali A., Limiti E., A novel monofilar-Archimedean metamaterial inspired leaky-wave antenna for scanning application for passive radar systems, *Microwave and Optical Technology Letters*, 60(8), 2055-2060, (2018).
- Alibakhshikenari M., Virdee B. S., Limiti E., Triple-band planar dipole antenna for omnidirectional radiation, *Microwave and Optical Technology Letters*, 60(4), 1048-1051, (2018).
- Alibakhshikenari M., Bal S. Virdee B. S., See, C. H., Abd-Alhameed R., Ali A., Falcone F., Limiti E., Wideband Printed Monopole Antenna for Application in Wireless Communication Systems, *IET Microwaves, Antennas & Propagation*, 12(7), 1222 – 1230, (2018).
- Alibakhshi-Kenari M., Naser-Moghadasi M., Sadeghzadeh R. A., Virdee B. S., Limiti E., Periodic Array of Complementary Artificial Magnetic Conductor Metamaterials-Based Multiband Antennas for Broadband Wireless Transceivers” *IET Microwaves, Antennas &*

- Propagation, 10(15), 1682 – 1691, (2016).
21. Alibakhshikenari M., Virdee B. S., See C., Abd-Alhameed R., Limiti E., Silicon-Based 0.450-0.475 THz Series-Fed Double Dielectric Resonator On-Chip Antenna Array Based on Metamaterial Properties for Integrated-Circuits, 13<sup>th</sup> International Congress on Artificial Materials for Novel Wave Phenomena – Metamaterials, Rome, Italy, 26-28, (2019).
  22. Alibakhshikenari M., Virdee B. S., Shukla P., See C., Abd-Alhameed R., Khalily M., Falcone F., Limiti E., Quazzane K., Parchin N., Isolation Enhancement of Densely Packed Array Antennas with Periodic MTM-Photonic Bandgap for SAR and MIMO Systems, *IET Microwaves, Antennas & Propagation*, 14(3), 183 – 188, (2020).
  23. Alibakhshikenari M., Virdee B. S., See C. H., Abd-Alhameed R., Ali, A. H., Falcone F., Limiti E., Study on Isolation Improvement Between Closely Packed Patch Antenna Arrays Based on Fractal Metamaterial Electromagnetic Bandgap Structures, *IET Microwaves, Antennas & Propagation*, 12(14), 2241 – 2247, (2018).
  24. Humble T. S., Thapliyal H., Munoz-Coreas E., Mohiyaddin F. A., Bennink R. S., Quantum Computing Circuits and Devices, *IEEE Design and Test*, 36(3), 69-94 (2019).
  25. Alibakhshikenari M., Virdee B. S., See C. H., Abd-Alhameed R. A., Falcone F., Limiti E., Energy Harvesting Circuit with High RF-to-DC Conversion Efficiency, 2020 IEEE International Symposium on Antennas and Propagation and North American Radio Science Meeting, Montréal, Québec, Canada, 1299-1300, (2020).
  26. Preskill J., Magnetic Monopoles, *Annual Review of Nuclear and Particle Science*, 34, 461-530, (1984).
  27. Liu Y., Yan H., Jia M., Du H., Du A., Zang J., Field-driven oscillation and rotation of multi-skyrmion cluster in a nanodisk, *Physical Review B*, 95(13), 134442, (2017).
  28. Bercini C., Fabri M., Homrich A., Vieira P., SUSY S-matrix Bootstrap and Friends, *Physical Review D* 101, 045022, (2020).
  29. Hermitian matrix, *Encyclopedia of Mathematics*, EMS Press, 2001, (1994).
  30. Ionescu L. M., Quantum Relativity, *General Physics*, arXiv:1005.3993, (2010).
  31. Hodge J. C., Magnetic field evolves to gravity field Part 1: Repulsion & Part 2: Particles, <http://intellectualarchive.com/?link=item&id=2164>, (2019).
  32. Jones-Smith K., Identifying quasi-particles using non-Hermitian quantum mechanics using PT quantum mechanics, *Philosophical Transactions - Mathematical, Physical and Engineering Sciences*, 371(1989), 1-14, (2013).
  33. Bender C. M., Making sense of non-Hermitian Hamiltonians, *Reports on Progress in Physics*, 70(6), (2007).
  34. Singh R. M., Real Eigenvalue of a Non-Hermitian Hamiltonian System, *Applied Mathematics*, 3, 1117-1123, (2012).
  35. Raes B., Cummings A. W., Bonell F., Costache M. V., Sierra J. F., Roche S., Valenzuela S. O., Spin precession in anisotropic media, *Physical Review B*, 95, 085403, (2017).
  36. Balaci O., Connection between Gravity and Electromagnetism, *Astronomical Review*, 8(4), 1-25, (2013).
  37. Marinescu D. C., Marinescu G. M., *Measurements and Quantum Information*, Ch. 2, 133-220, (2012).
  38. Datta N., Mathematical Statistical Physics: 4.0.2 Reduced density matrix and partial trace, in *Les Houches*, 83.1-816, <https://www.sciencedirect.com/topics/mathematics/reduced-density-operator>, (2006).
  39. Weissbluth M., Density Matrices: 13.7 Fock-Dirac Density Matrices, in *Atoms and Molecules*, Ch. 13, 268-289, (1978).
  40. Müller M., ... Zoller P., 3.4.3 Topological Order in Density Matrices, in *Advances Atomic, Molecular, and Optical Physics*, (2012).
  41. Fujimura Y., Lin S. H., Multiphoton Spectroscopy: II. D Density Matrix Method, in *Encyclopedia of Physical Science and Technology*, Third Edition, 199-229, (2003).
  42. Landau L. D., Lifshitz E. M., The Basic Concepts of Quantum Mechanics: §7. The density matrix, in *Quantum Mechanics: A Shorter Course of Theoretical Physics*, Ch. 1, 3-27, (1974).
  43. Chandra N., Parida S., Quantum Entanglement in Photon-Induced Electron Spectroscopy of Atoms and Molecules: Coulombic Density Matrix for 2-DPI, in *Advances in Imaging and Electron Physics*, (2016).
  44. Schadschneider A., ... Nishinari K., Methods for the Description of Stochastic Models: 2.6.3 Density-Matrix Renormalization Group, in *Stochastic Transport in Complex Systems*,

- Ch.2, 27-70, (2011).
45. Datta N., *Mathematical Statistical Physics: Quantum states and density matrices*, in Les Houches, 83.1-816, <https://www.sciencedirect.com/topics/mathematics/density-matrix>, (2006).
  46. Alibakhshi-Kenari M., *Design and Modeling of New UWB Metamaterial Planar Cavity Antennas with Shrinking of the Physical Size for Modern Transceivers*, *International Journal of Antennas and Propagation*, 2013(11), 1-12, (2013).
  47. Lattanzi R., Wiggins G. C., Zhang B., Duan Q., Brown R., Sodickson D. K., *Approaching ultimate intrinsic signal-to-noise ratio with loop and dipole antennas*, *Magnetic Resonance in Medicine*, 79(3), 1789-1803, (2018).
  48. Barceló C., Carballo-Rubio R., Garay L. J., Jannes G., *Electromagnetism as an emergent phenomenon: a step-by-step guide*, *New Journal of Physics*, 16, 123028, (2014).
  49. Su S. Q., Wu S. Q., Hagihala M., Miao P., Tan Z., Torii S., Kamiyama T., Xiao T., Wang Z., Ouyang Z., Miyazaki Y., Nakano M., Nakanishi T., Li J. Q., Kanegawa S., Sato O., *Water-oriented magnetic anisotropy transition*, *Nature Communications*, 12, 2738, (2021).
  50. Illge, R., Wünsch V., *Relativistic Wave Equations Including Higher Spin Fields: Wave Equations for Low Spin in Minkowski spacetime*, in *Encyclopedia of Mathematical Physics*, [https://www.wizdom.ai/publication/10.1016/B0-12-512666-2/00161-9/title/relativistic\\_wave\\_equations\\_including\\_higher\\_spin\\_fields](https://www.wizdom.ai/publication/10.1016/B0-12-512666-2/00161-9/title/relativistic_wave_equations_including_higher_spin_fields), (2006).
  51. Marinescu D. C., Marinescu G. M., *Preliminaries*, in *Classical and Quantum Information*, Ch.1, 1-131, (2012).
  52. Brini E., Fennell C. J., Fernandez-Serra M., Hribar-Lee B., Lukšič M., Dill K. A., *How Water's Properties Are Encoded in Its Molecular Structure and Energies*, *Chemical Reviews*, 117(19), 12385–12414, (2017).
  53. Rajantie A., *The search for magnetic monopoles*, *Physics Today*, 69(10), 40-46, (2016).
  54. *Bohr's Atom*, *Modern Physics*, [https://strings.lums.edu.pk/home/wp-content/uploads/2016/01/Solution\\_Homework-3-16.pdf](https://strings.lums.edu.pk/home/wp-content/uploads/2016/01/Solution_Homework-3-16.pdf), (2016).
  55. Griffiths D. J., *Introduction to Quantum Mechanics*, Prentice-Hall, ISBN 0-13-124405-1, 155, (1995).
  56. 6.2 The Bohr Model, *CHEMISTRY*, [https://openstax.org/books/chemistry-2e/pages/6-2-](https://openstax.org/books/chemistry-2e/pages/6-2-the-bohr-model)  
[the-bohr-model](https://openstax.org/books/chemistry-2e/pages/6-2-the-bohr-model).
  57. Bialynicki-Birula I., Bialynicka-Birula Z., *Time crystals made of electron-positron pairs*, *Physical Review A* 104, 022203, (2021).
  58. Auletta G., Fortunato M., Parisi G., *Quantum Mechanics Into a Modern Perspective*, pages 756, ISBN 978-0-521-86963-8, Cambridge University Press, (2009).
  59. Markoulakis E., Chatzakis J., Konstantaras A., Antonidakis E., *A synthetic macroscopic magnetic unipole*, *Physica Scripta*, 95(9), 095811, (2020).
  60. Vepsäläinen A.P., Karamlou A.H., Orrell J.L., et al., *Impact of ionizing radiation on superconducting qubit coherence*, *Nature*, 584, 551-556, (2020).
  61. Broholm C., *Basic Research Needs Workshop on Quantum Materials for Energy Relevant Technology*, <https://www.energy.gov/science/bes/basic-energy-sciences>, (2016).
  62. *The Physics of Magnetic Monopoles - with Dr. Felix Flicker*, The Royal Institution, You-tube video sponsored by the New College, Oxford, hosted by Prof. Daniela Bortoletto, (2020).
  63. Matos T., Gomez E., *Space-Time Curvature Signatures in Bose-Einstein Condensates*, *The European Physical Journal D*, 69(5), (2015).
  64. Hossenfelder S., *Interpretation of Quantum Field Theories with a Minimal Length Scale*, *Physical Review D*, 73, 105013, (2006).
  65. O'Neill C. C., *publication group references:*
  66. O'Neill C.C., *Magic Squares, the Weak Force and the Higgs Mechanism*, [https://www.researchgate.net/publication/350123517\\_Magic\\_Squares\\_the\\_Weak\\_Force\\_and\\_the\\_Higgs\\_Mechanism](https://www.researchgate.net/publication/350123517_Magic_Squares_the_Weak_Force_and_the_Higgs_Mechanism), (2021).
  67. O'Neill C.C., *Magic Squares and Planck's Constant*. [https://www.researchgate.net/publication/350323945\\_Magic\\_Squares\\_and\\_Planck's\\_Constant](https://www.researchgate.net/publication/350323945_Magic_Squares_and_Planck's_Constant), (2021).
  68. O'Neill C.C., *The Weak Force & Magic Square Order 6*, [https://www.researchgate.net/publication/351603528\\_The\\_Weak\\_Force\\_Magic\\_Square\\_Order\\_6](https://www.researchgate.net/publication/351603528_The_Weak_Force_Magic_Square_Order_6), (2021).
  69. O'Neill C.C., *Finite Field Construction of Odd Order Magic Squares*, [https://www.researchgate.net/publication/350157391\\_Finite\\_Field\\_Construction\\_of\\_Odd\\_Order\\_Magic\\_Squares](https://www.researchgate.net/publication/350157391_Finite_Field_Construction_of_Odd_Order_Magic_Squares), (2021).
  70. O'Neill C. C., *Octonions, The Three Flavours of Matter And A New Kind of Super-Symmetry*,

- Canadian Journal of Pure and Applied Sciences*, 15(2), 5261-5268, (2021).
71. O'Neill C. C., 24-cell & the Standard Model, [https://www.researchgate.net/publication/349896140\\_24-cell\\_the\\_Standard\\_Model?channel=doi&linkId=60513680299bf173674adc0b&showFulltext=true](https://www.researchgate.net/publication/349896140_24-cell_the_Standard_Model?channel=doi&linkId=60513680299bf173674adc0b&showFulltext=true), (2021).
  72. O'Neill C. C., A Complementary Geometric Explanation of the 3 Flavours, [https://www.researchgate.net/publication/349376074\\_A\\_Complementary\\_Geometric\\_Explanation\\_of\\_the\\_3\\_Flavours](https://www.researchgate.net/publication/349376074_A_Complementary_Geometric_Explanation_of_the_3_Flavours), (2021).
  73. O'Neill C. C., The Graviton As 5D Chamfered Cube, [https://www.researchgate.net/publication/348355596\\_The\\_graviton\\_as\\_5d\\_chamfered\\_cube](https://www.researchgate.net/publication/348355596_The_graviton_as_5d_chamfered_cube), (2021).
  74. O'Neill C. C., Making Sense Of The Standard Model, [https://www.researchgate.net/publication/349110442\\_Making\\_sense\\_of\\_the\\_standard\\_model](https://www.researchgate.net/publication/349110442_Making_sense_of_the_standard_model), (2021).
  75. O'Neill C. C., Reimagining Complex Numbers. *Canadian Journal Of Pure And Applied Sciences*, 15(2), 5201-5219, (2021).
  76. O'Neill C. C., A Non-Relativistic Reinterpretation Of Particle Spin, [https://www.researchgate.net/publication/351785566\\_A\\_non-Relativistic\\_reinterpretation\\_of\\_particle\\_spin](https://www.researchgate.net/publication/351785566_A_non-Relativistic_reinterpretation_of_particle_spin), (2021).
  77. O'Neill C. C., Clifford-Like Rotations Of Possible Dark Matter Particles, And A More Beautiful Theory, [https://www.researchgate.net/publication/352845416\\_Clifford-Like\\_rotations\\_of\\_possible\\_dark\\_matter\\_particles\\_and\\_a\\_more\\_beautiful\\_theory](https://www.researchgate.net/publication/352845416_Clifford-Like_rotations_of_possible_dark_matter_particles_and_a_more_beautiful_theory), (2021).
  78. Jensen H., Subtle Relations: Prime Numbers, Complex Functions, Energy Levels And Riemann, [https://www.imperial.ac.uk/~Hjens/Riemann\\_talk.pdf](https://www.imperial.ac.uk/~Hjens/Riemann_talk.pdf) Article.
  79. <https://stackoverflow.com/questions/49803366/Point-Opacity-Relative-To-Depth-Matplotlib3d-Point-Plot>.
  80. 4D Flat Spacetime, P.19, [https://www.mv.helsinki.fi/Home/Syrasane/Cosmo/Lect2018\\_02.Pdf](https://www.mv.helsinki.fi/Home/Syrasane/Cosmo/Lect2018_02.Pdf).
  81. Tesh S., Flash Physics: Sandra Faber Wins Gruber Prize, Transforming Magnetic Monopoles, Vacuum Scattering Revealed, *Cosmology News*, <https://Physicsworld.com/A/Flash-Physics-Sandra-Faber-Wins-Gruber-Prize-Transformingmagnetic-Monopoles-Vacuum-Scattering-Revealed>, Sarah Tesh Is Features' Editor Of Physics World, (2017).
  82. Iyer R., Absolute Genesis Fire Fifth Dimension Mathematical Physics, Engineering International Publisher with Amazon.com, ISBN 978-0970689801, (2000).
  83. Malaver M., Kasmaei H., Iyer R., Sadhukhan S., Kar A., A theoretical model of Dark Energy Stars in Einstein-Gauss-Bonnet Gravity, *Applied Physics*, 4(3), 1-21, (2021).
  84. Lenstra A., Integer Factoring, *Designs Codes and Cryptography*, 19, 101-128, (2000).
  85. Schiller J., Quantum Computers, ISBN 9781439243497, (2009).
  86. Zyga L., Fibonacci quasiparticle could form basis of future quantum computers, <https://phys.org/news/2014-12-fibonacci-quasiparticle-basis-future-quantum.html>, (2014).
  87. Quesnel N., Quantum Computing Cooling, <https://www.qats.com/cms/2019/08/02/quantum-computing-cooling>, (2019).
  88. Grumbling E., Horowitz, M., Quantum Computing Progress and Prospects, A Consensus Study Report of images, The National Academies Press, Washington, DC, <http://www.nap.edu>, Chapter 2 Quantum Computing: A New Paradigm, ISBN-13: 978-0-309-47969-1, 2019.
  89. Lendinez S., Jungfleisch M. B., Magnetization dynamics in artificial spin ice, *Journal of Physics Condensed Matter*, 32(1), 013001, (2020).
  90. Meitner L., Hahn O., in *Berlin Experimental Reports 2009*, Helmholtz-Zentrum Berlin, edited by A. Rodig, A. Brandt, and H. A. Graf, <https://www.helmholtz-berlin.de>, ISSN:1868-5781, (2010).